Vital Annex: International Journal of Novel Research in Advanced Sciences
ISSN: 2751-756X
Volume 04 Number 03 (2025)
https://innosci.org/IJNRAS

Article

STRUCTURAL AND ELECTRICAL INVESTIGATION OF POROUS GaAS LAYERS PREPARED BY LASER-INDUCED ETCHING METHOD.

Hassan A. Kadhem[1] Abdul Hakim Sh. Mohammed[2]

1. Ministry of Education, Open Educational College, Kirkuk Center,iraq, albayaty.hassan1@yahoo.com
2. Department of Physics, college of Education for pure sciences, University of Kirkuk, Kirkuk, Iraq, hakimsh@uokirkuk.edu.iq

* Correspondence: albayaty.hassan1@yahoo.com

Abstract: in this study, a laser induced etching technique was used to create layers of porous GaAs on a donor GaAs wafer with orientation (111) and resistivity equal to2.45 x 10-3 ohm. Cm. The process involved focusing a beam of (1050nm) Diode laser with power densities of (0.5, 3, 6, 9) W/cm2 incident onto the samples. The samples were immersed in hydrofluoric acid with 40% concentration for constant etching time of 50 min. an Atomic Force Microscope (AFM) was used to investigate porous GaAs layers, which showed the formation of nano-sized particles on the surfaces of all samples, with sizes varying from 15.7310 nm to 3.47124 nm, increasing in porous layer thickness from 2nm to 81.03 nm with increasing laser power from 0.5 to 9 W/cm2. The results of the electrical properties of Al/porose-GaAs/n- GaAs/Al devices in the forward bias showed an improvement in the rectification properties with increasing laser power, In reverse bias, the current-voltage curve does not show any saturation state due to the effect of both electric and thermal fields on the height of the effective barrier. Calculated values of ideality factor for all diodes showed close to unity.

Keywords: Porous GaAs, GaAs nanostructures , electrical measurements, Atomic force microscopy, laser induced etching,

Citation: Kadhem, H, A, Structural And Electrical Investigation of Porous GaAs Layers Prepared by Laser-Induced Etching Method. Vital Annex: International Journal of Novel Research in Advanced Sciences 2025, 4(3), 89-105.

Received: 10th Jan 2025
Revised: 11th Jan 2025
Accepted: 24th Jan 2025
Published: 27th Mar 2025

1. Introduction

GaAs nanostructures are increasingly being used in various applications such as optoelectronic devices [1], light emitting diodes [2], solar cells [3], Tunnel field effect transistors [4], hydrogen-sensing [5, antireflective coating for solar cells[6], thermoelectric devices [7]. GaAs nanostructures can be produced by several techniques, including: chemical. [8], physical [9], electrochemical etching techniques [10].and can be produced in different shapes and forms such as nanowires. [11], quantum wells [12] , nanodisks [13], coupled ring/ disks [14], nano-conical [15], quantum dots [16], quantum dashes [17], quantum rings [18] , nanopores [19], and nanoholes [20] . It was observed that the porosity, porous layer structure , dimensions of the pores depend on the doping density and the crystal orientation, and independent on the applied current. [21,22]. Many studies have been presented on the preparation of Porous GaAs, laser induced etching technique using

Nd:YAG (1060 nm) is one of them [23][24][25][26] .in this study we used the same technique with a diode laser of (1050nm) wavelength to produce porous GaAs samples.

Laser-induced etching mechanism; Electron-hole pairs are generated as a result of illumination of the GaAs surface. The holes are drifted under the influence of the electric field at GaAs/electrolyte interface Thus, etching begins through the redox process ,the above chemical reactions can be given [27,28] by

$$GaAs + 6h^+ \rightarrow Ga^{3+} + As^{3+} \quad (1)$$

$$GaAs + 3e^- \rightarrow Ga^0 + As^{3-} \quad (2)$$

The holes move towards the surface due to band bending in the space charge region where the etching process begins ,then the formation of pits in GaAs. The basic condition for pore formation is the initiation of the etching process. The pit is formed on the surface of GaAs at the point where the dislocation rate is highest. The dislocation density of GaAs ranges from medium to high even at its highest purity.[29] Surface intersection lead to more free bonds forming, Then there is an increase in chemical activity at surface defects and localized etching induces a pit, The spread and expansion of the pore size results from the increase in the electric field strength at the tip of the pits [30]. The flow of carriers across the electrolyte / GaAs surface controls the dissolution process.

2. Materials and Methods

2.1. Laser–Induced Etching process: The Starting material of the prepared samples was a commercially available (111) oriented n-type GaAs:Te wafers (500μm) thickness with resistivity of 2.45×10^{-3} ohm. cm which corresponds to doping concentration of about 8.21×10^{17} cm^{-3} , cutted into pieces of (0.7cm x0.7cm) , After cleaning the samples with acetone and ethanol, they were placed for 5 seconds in HF acid at a concentration of %5 to remove the native oxide layer. The samples were placed on U-shaped Teflon supports inside a container of the same material filled with 40% HF acid for etching time (50) min. a diode laser of a wavelength (1050nm) (DLN-1050-MADE IN BELARUS) in CW mode with an output power of 5 W and rectangular beam (2cm x3cm) Figure (1 a,b) was used to perform laser – induced etching process, It is worth noting that the laser has a wavelength of 1050 nm, which is within the infrared (invisible) region, but when using a mobile phone camera, it is possible to photograph the light spot of the laser). (Two-channel DUO laser power meter (gentec) was used to measure the laser power density. Diode laser beam was focused to a circular spot with different diameters by using different focal length Lenses to get required power density of (0.5 ,3 , 6. 9) W/cm^2 on the mirror–like surface of the samples. Figure (1. c). Figure (1. d) shows the schematic diagram of the experimental set-up for the laser-induced etching system which used for studying the effect of laser power density on the properties of produced GaAs nanocrystallites layers. After the etching process was completed, the samples were removed from the Teflon container and placed in plastic containers filled with methanol In order to be ready to study the morphological characteristics of the porous GaAs layer, as well as prepare it for the deposition of aluminium thin films and conduct a study of the electrical properties of the manufactured Al/ Pourse- GaAs / n-GaAs /Al devices.

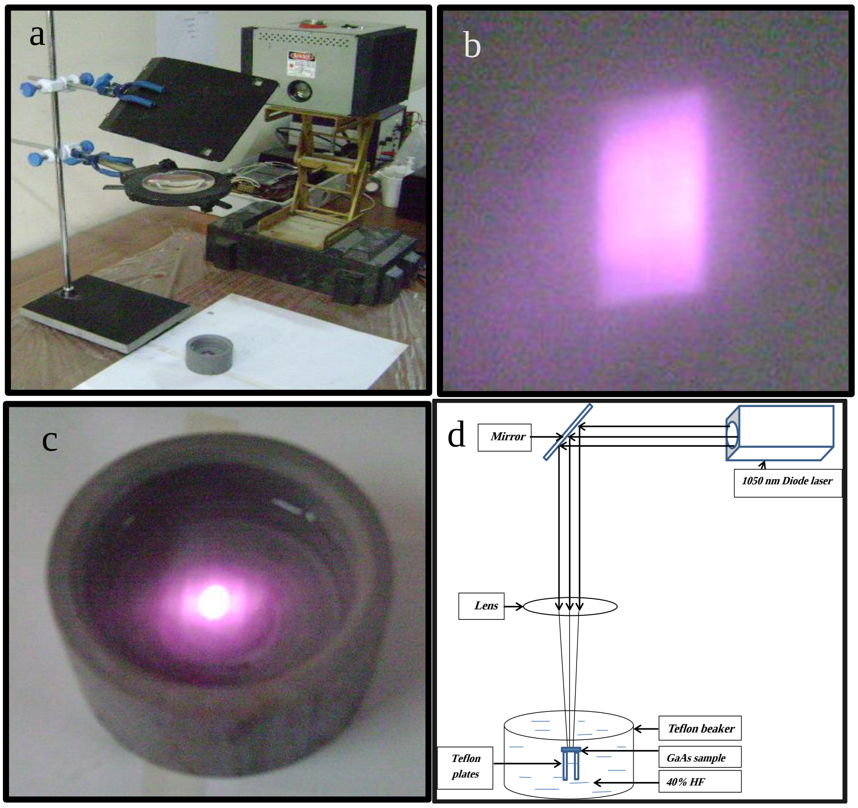

Figure (1) :(a) a photograph of the experimental set-up. (b) rectangular laser beam (c) GaAs sample inside Teflon vessel with laser spot on it (d) a schematic diagram of the experimental set-up.

2.2 Metallization: After etching process, a thin layer of high-purity aluminium (99.999%) with a thickness of 200 mm was deposited on both sides (the porous side and the bulk side) of the prepared samples to make the electrical contacts, by means of thermal evaporation methods, using Edward,s type E306A unit, Silver paste was used to connect the copper wires on the surface of the samples. A Kiethley-616 electrometer was used to record the I(V) curve in Al/ Porous- GaAs / n-GaAs /Al devices.

3. Results and discussion

3.1. Microstructural characterization: An atomic force microscope was used to study the morphology of the porous GaAs layers, using a scanning area of (0.78µm x 0.78µm). The porous GaAs layers that formed on the surfaces of samples were prepared on (1 1 1) n-type GaAs by using a (1050nm) diode laser for etching proses in HF acid of 40% concentration for a fixed irradiation time of 50 min , with different power densities of (0.5, 3, 6, 12) W/cm2. Figures (2,3,4,5) shows Changes in the morphology of the etched surfaces (particle sizes, porous layer thickness, statistical distribution of these particles, RMS roughness and Maximum height). Figure (2a) shows AFM image of the three-dimensional configuration of the porous GaAs sample prepared at power density of o.5 W/ cm2 . The porous GaAs layer shows formation of nanostructured particles have an average size of about 15.731 nm, The main root square of the roughness (RMS roughness) was 2.10983nm, Figure 2b shows the morphology of the porous layer in two dimensions. The statistical distribution of the sizes of these nanoparticles is shown in Figure 2c. We notice that the particle sizes range from zero to about 52nm,and the particles whose sizes are between7.5 nm and 10 nm are the most numerous, the Extracted Profile shows in figure 2(d), rise and fall of particles from zero level, where particles from zero to 0.7 appear to be at a low level, and they begin to be counted as rising up especially after 0.9 to 1 micrometer, the height of particles above zero increases significantly, In general, the layer thickness of this sample can be considered close to 2nm figure 2(e). The failure to form a porous layer with a clear thickness can be explained by the weak laser power density, as the chemical dissolution process was limited to a thin layer on the surface of the sample only.

As the laser power density increased to 3 W/cm2, the particles became smaller in size, 4.6096 nm, as well as in surface roughness, 1.20819 nm. Figure 3 (a , b). the statistical distribution of nanoparticles on the surface is shown in the figure (3c), where the particle sizes range from 0 to 33nm, forming two groups. The first starts from a size of zero up to approximately 14nm, the center of this group is 8.34nm, the second group is from 14 to 33nm, and the center of this group is at 26nm. Figure (3d) shows the height profile of the particles, where the height of the formed nanoparticles is above the level of 10 nm, and gradually decreases until 0.6 μm, after which it decreases to a minimum value of -10 nm at the distance of 0.9μm. It is observed in Figure 3(e) that the thickness of the porous layer is about 0.33.34nm.

The nanoparticles formed on the surface of the sample that was etched using a power density of 6 W/ cm2, showed a particle size of 4.6013 nm, RMS roughness surface of 1.19678 nm, Figure 4(a,b) . The statistical distribution of particle sizes on the surface showed three groups based on size. The first category is for particles whose sizes range from zero to 10 nm, the second group is between 10 nm and 25 nm. In the middle of this category, the highest percentage of particles is found, while the third category is between 25 nm and 59 nm. figure 4(c). It is noted that Producing more aggregates of particles with increasing laser power, The surface level for this sample showed a clear decrease at zero micrometers, with a depth of more than 20 nm . It begins to approach the zero level at 0.6 micrometers, then begins to gradually rise to more than 30 nm at one micrometer, with a porous layer thickness of 66.86nm, figure 4(d and e).

The nanoparticles formed on the surface of the sample were the smallest in size. (3.47124nm) in which the laser induced etching process was performed using a power density of 9 W/ cm2 . The main root square of the roughness (RMS roughness) was 711.232 pm , Figure 5 (a,b) . The statistical distribution of surface particles showed five categories of aggregates based on their sizes and the centers of the categories were (3 ,14, 23, 30, 47) nm and their percentages as shown in the figure 5 (c) . The rise and fall of particles below the zero level (Extracted Profile) is shown in the figure 5(d) , as the particles below the zero level at about 20 nm at 0 micrometers begin to rise gradually to reach the zero level at 0.6 micrometers, then they rise to reach about 60 nm at the 1 micrometer, forming a porous layer with a thickness of 81.03 figure 5 (d and e)

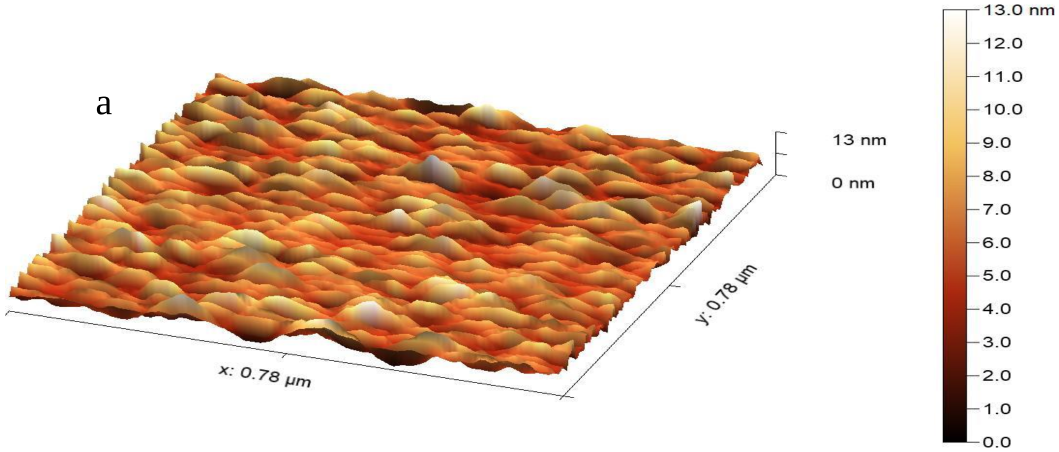

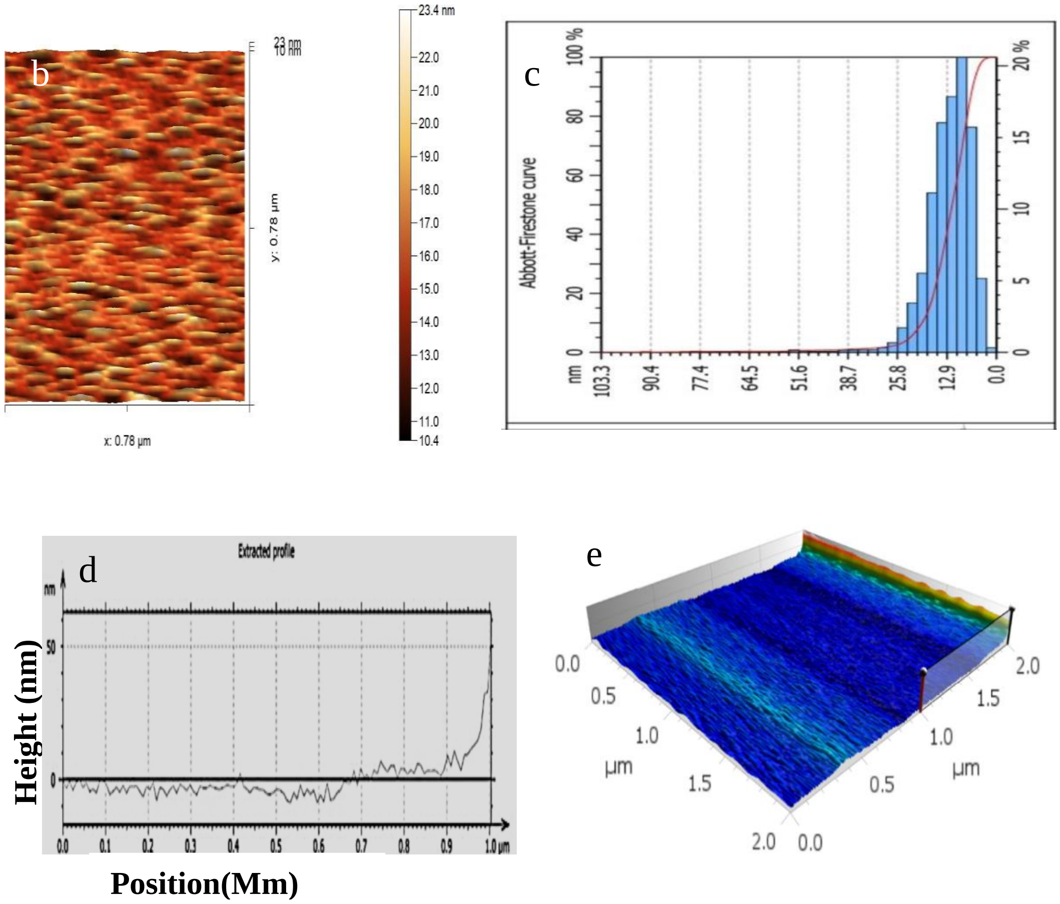

Figure (2) (a)AFM images of the three-dimensional configuration of the porous GaAs samples prepared by laser induced etching method using a diode laser (1050 nm) with laser power density of o.5 W/cm2 (b) two-dimensional AFM images (c) The statistical distribution of the nanoparticles formed on the surface of the sample , (d) 2-D Extracted Profile.(e) porous layer thickness .

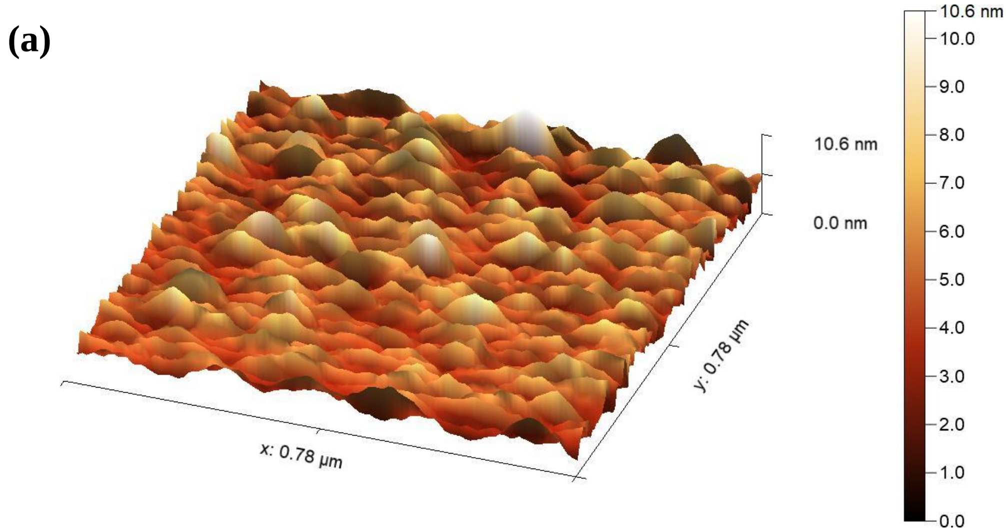

(b)

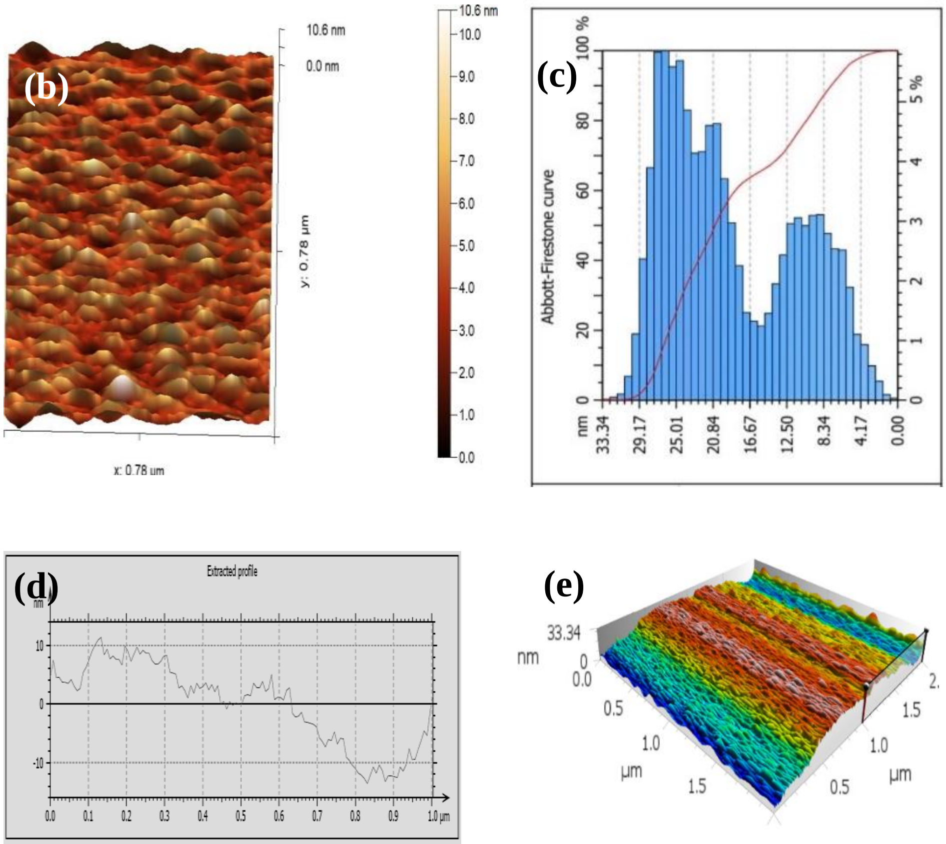

Figure (3) (a)AFM images of the three-dimensional configuration of the porous GaAs samples prepared by(1050 nm) diode laser induced etching method with laser power density of 3 W/cm2 (b) two-dimensional AFM images (c) The statistical distribution of the nanoparticles formed on the surface of the sample in figure (3a), (d) Extracted Profile (e) porous layer thickness .

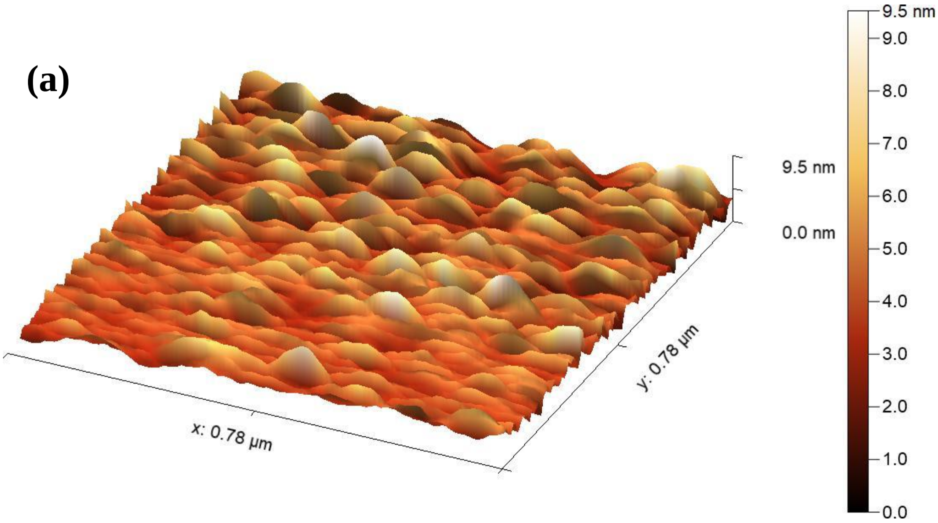

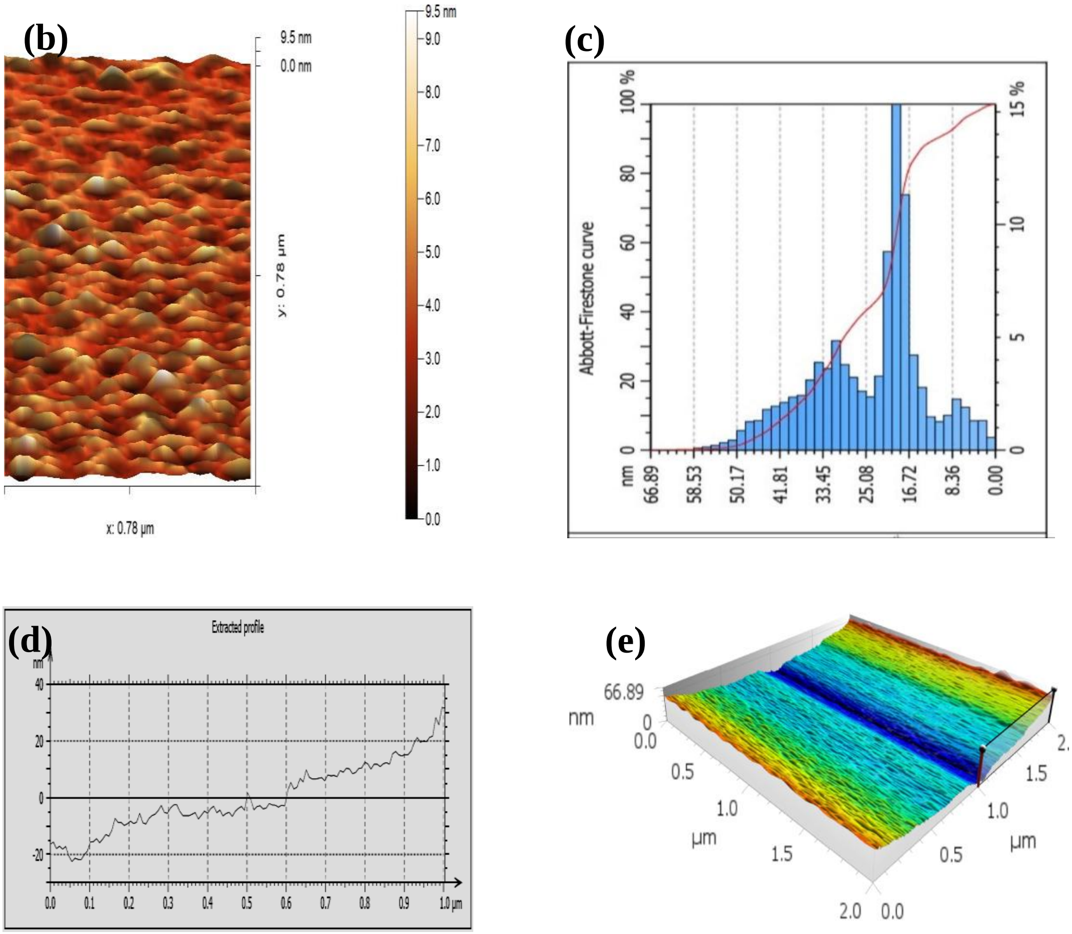

Figure (4) (a)AFM images of the three-dimensional configuration of the porous GaAs samples prepared by(1050 nm) diode laser induced etching method with laser power density of 6 W/cm2 (b)AFM images in two-dimensional (c) The statistical distribution of the nanoparticles formed on the surface, (d) Extracted Profile (e) porous layer thickness.

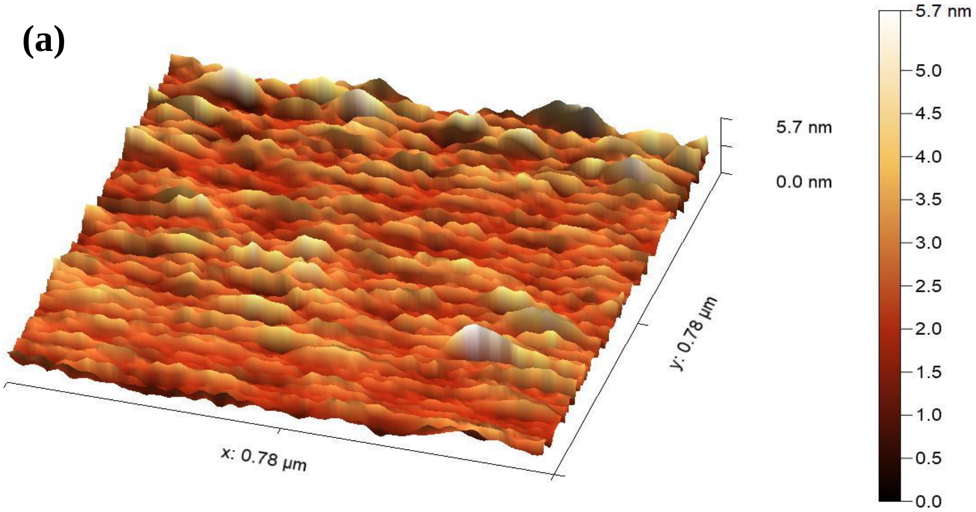

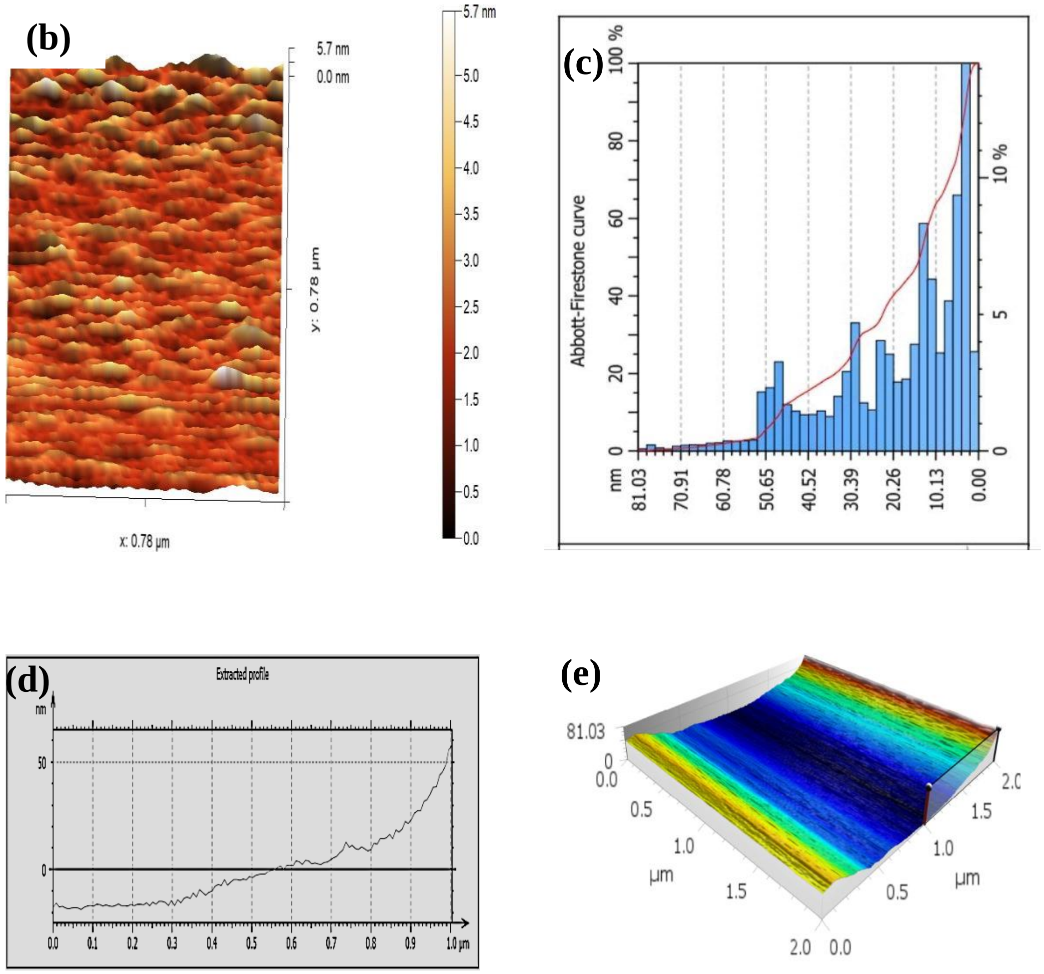

Figure (5): (a)AFM images of the three-dimensional configuration of the porous GaAs samples prepared by laser induced etching method using (1050 nm) diode laser power density of 9 W/cm2 (b)AFM images in two-dimensional (c) The statistical distribution of the nanoparticles formed on the surface, (d) Extracted Profile (e) porous layer thickness .

The above results are arranged and explained in the table (1) and figures (6 & 7).

Table (1) shows the most important morphology results

Laser power density W/cm^2	porous layer thickness (nm)	Average value (nm)	RMS roughness (Sq) (nm)	Maximum height (Sz)(nm)
0.5	2	15.7310	2.10983	39.1660
3	33	4.6096	1.20819	11.4607
6	66	4.6013	1.19678	14.9311
9	81	3.47124	0.711232	7.78178

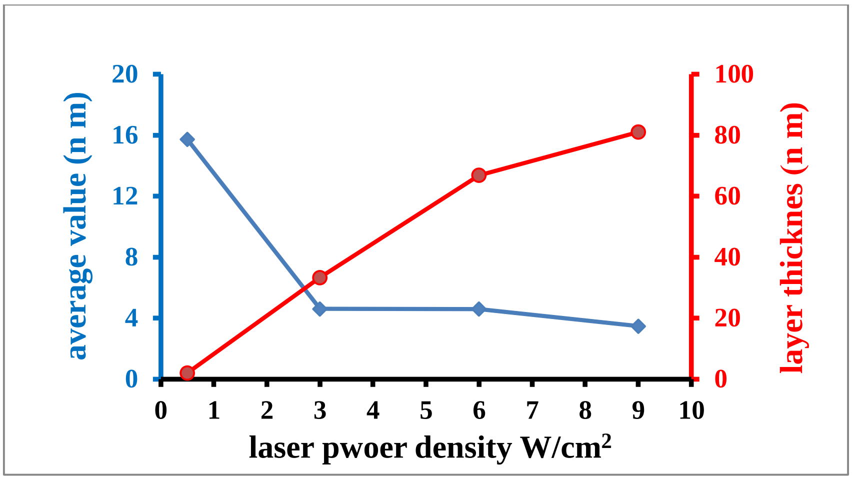

Figure (6). The thickness (red line) and average nano particles values at each laser power density.

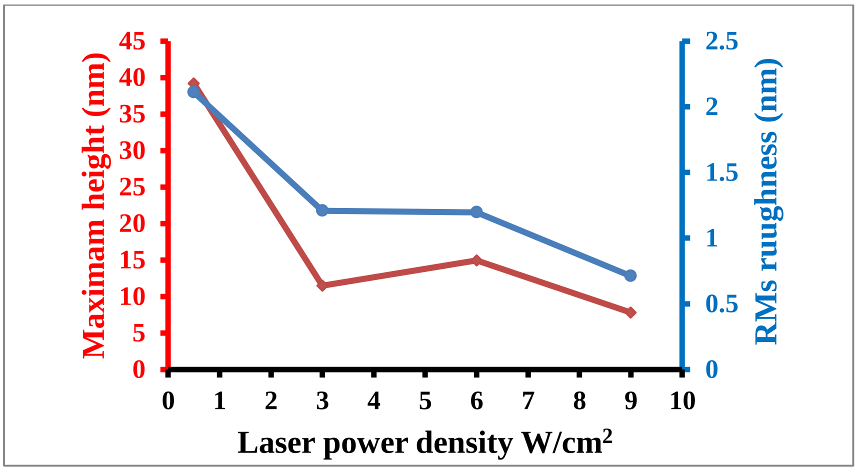

Figure (7). The Maximum height (red line) and RMS roughness (Sq) (nm) at each laser power density.

3.2 Current–Voltage Characteristics

The Studies presented in explaining the electrical properties and The electronic transport mechanism in metal/porous GaAs/n-GaAs/metal [31][32][33],have relied that, The current-voltage characteristics in forward bias depend on trap-assisted space charge limited conduction ,While in reverse voltage , the carriers transport across the interface between the bulk layer and the porous layer by thermionic emission. In the high voltage region, most of the traps will be occupied with injected carriers.[34]

The results of the current-voltage (I-V) measurements at room temperature in forward and reverse I–V curves of the fabricated devices of Al/Porous GaAs /n-GaAs/Al structures are shown in Figure (8). We notice that the rectification behaviour improves with increasing of laser power densities, This behaviour is expected when we observe the changes in the surface morphologies for samples in Figure (2,3,4and 5). Changes in particle size where the average particle size decreased from 15.733 nm to 3.41724 nm and the thickness of the porous layer increased from 2 nm to 81.03 nm with increasing the laser power from 0.5 to 9 w/cm2 respectively. Increasing the laser power during preparation led to the generation of more holes that enhanced the chemical dissolution process, thus increasing the porosity in the upper layer exposed to the laser beam. As a result of this process, during electrical connection, the injected carriers in the porous layer are depleted due to the formation of traps that capture these carriers, This leads to the formation of a heterojunction between the porous layer, which is less negative, and the highly negative bulk layer (substrate). From Figure 8,We notice also that there is no saturation current in the reverse bias , but shows voltage dependence. Indicates the transport of carrier through a heterostructure. This nonlinear relationship between the current and voltage at temperature T can be written as;

$$I = Is \ e^{\frac{q(V-R_S I)}{nK_B T}} \left[1 - e^{\frac{q(V-R_S I)}{nK_B T}}\right] \qquad (5)$$

where q is the electron charge, V is the applied bias, n the ideality factor, kB the Boltzmann constant, T the temperature. Is is the saturation current given by

$$Is = A^* A \, T^2 \, e^{-\frac{E_b}{K_B T}} \qquad (6)$$

$$A^* = A \, \frac{m^*}{m_e} \qquad (7)$$

where A the effective diode area, A* is the n doped GaAs effective Richardson constant given by A* = 8.16 Acm-2K-2 and Eb is the zero bias effective barrier height. [31]. The formula for Equation 5 includes the influence of the transport mechanisms in the depletion region due to the thermionic field emission and the electron-hole pairs recombination. Equation (5) is reduced to the law governing diffusion current due to thermionic emission for n = 1 and Rs=0. Then, The most efficiency of the factor

[(1 - exp(- qV/kT)] is in the reverse bias region and also when the regime is up to 3 kT/q in forward bias . The relationship is important from a physical point of view because the factors responsible for the non-ideal behavior under forward bias are active under reverse bias.[32] The suggested mechanism under forward bias behavior is based on limited conduction current of the space-charge. To determine how the charges transporting through the Al/porous-GaAs/n-GaAs/Al structures, we show in Fig. 9 semi - logarithmic forward current–voltage plots for each sample. It is noted that the characteristics show a behavior similar with that reported by [31,33] for similar devices.

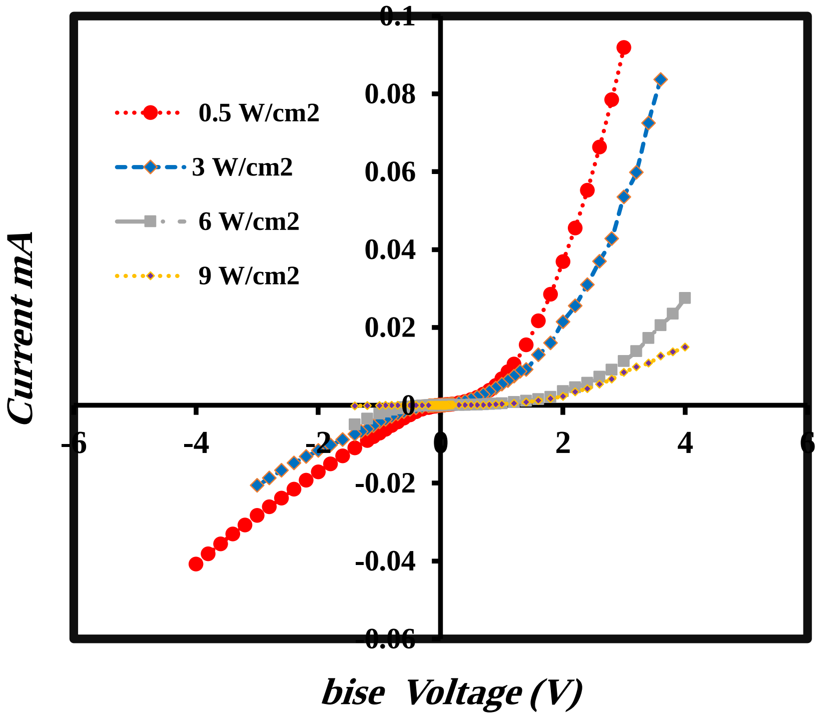

Figure (8); Dependence on laser power densities of the current–voltage characteristics of Porous GaAs samples prepared by (LIE) technique, etched with (0.5,3,6,9) W/cm2

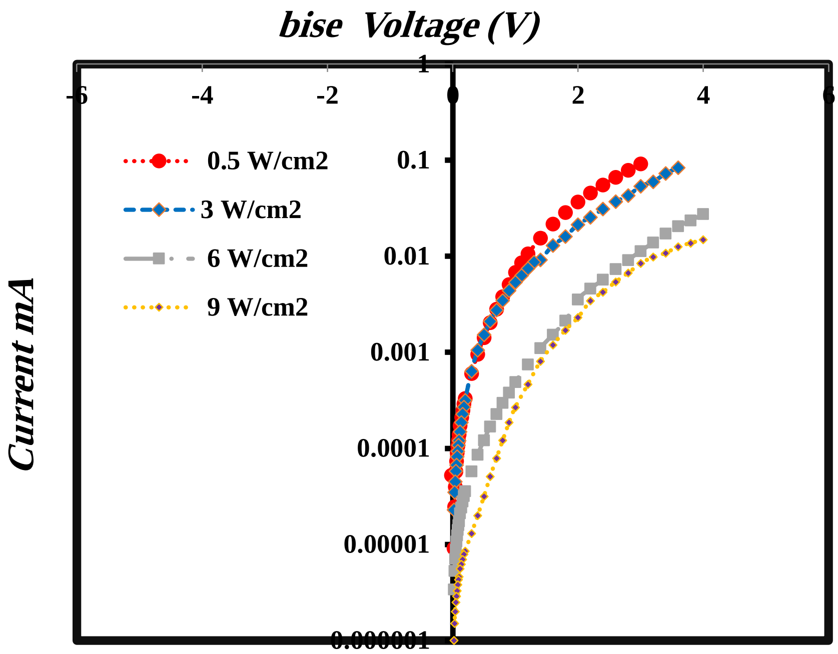

Figure (9): semi- logarithmic forward bias I–V plots for the Al / Porous GaAs / n-GaAs/ Al structures fabricated by porous- GaAs samples etched at deferent laser power densities (0.5,3,6,9) W/cm2 .

Equation (5) can be written as follows:

$$\frac{I}{\left(1-e^{i\frac{q(V_i-IR_s)}{kT}}\right)}=I_s e^{\frac{q(V_i-IR_s)}{nkT}} \qquad (8)$$

Taking ln for each side of eq. (8), we get eq. (9), comparison it with linear eq.(10), we can obtain the value of slope (m) in eq.(11), and the value of ideality factor n from eq.(12)

$$\ln\frac{I}{\left(1-e^{i\frac{q(V_i-IR_s)}{kT}}\right)}=\ln I_s+\frac{q}{nkT}\left(V_i-IR_s\right) \qquad (9)$$

$$y=b+mx \qquad (10)$$

$$m=\frac{q}{nkT} \qquad (11)$$

$$n=\frac{q}{mkT} \qquad (12)$$

Table (2) shows the calculation of the ideality factor by substituting the current and voltage values into Equations (9). The slope values calculated from Figure 10 and substituted into Equation 12 to calculate the ideality factor values for each Al/pours –GaAs / n-GaAs/Al diodes , , their porous layers were prepared using laser densities of (a) 0.5

w/cm2 (b) 3 w/cm2 (c) 6 w/cm2 (d) 9 w/cm2, Schottky diodes from the reverse bias I–V data shown in Fig8.

(a) 0.5 w/cm^2

bias (volt)	I (mA)	$ln(\frac{-I}{1-e^{\left(\frac{-qV}{K_BT}\right)}})$	Slope (m)	$n = \frac{q}{slope.K_BT}$
-0.1	-0.000245	$\ln(\frac{-245 * 10^{-9}}{1-e^{\left(\frac{-1.602*10^{-19}*(-0.1)}{1.38*10^{-23}*300}\right)}})$ = -19.06	37.602	1.0127
-0.5	-0.00249	-32.199		
-1	-0.00716	-50.5		
-2	-0.01715	-88.2		

(b) 3 w/cm^2

bias (volt)	I (mA)	$ln(\frac{-I}{1-e^{\left(\frac{-qV}{K_BT}\right)}})$	Slope (m)	$n = \frac{q}{slope.K_BT}$
-0.1	-0.000066	-20.37	37.15	1.0403
-1	-0.00428	-51.01		
-2.4	-0.0148	-103.8		
-3	-0.0206	-127.97		

bias (volt)	I (mA)	$ln(\frac{-I}{1-e^{\left(\frac{-qV}{K_BT}\right)}})$	Slope (m)	$n = \frac{q}{slope.K_BT}$
-0.1	-0.000066	-20.37	37.15	1.0403
-1	-0.00428	-51.01		
-2.4	-0.0148	-103.8		
-3	-0.0206	-127.97		

(c) 6 w/cm^2

bias (volt)	I (mA)	$ln(\frac{-I}{1-e^{\left(\frac{-qV}{K_BT}\right)}})$	Slope (m)	$n = \frac{q}{slope.K_BT}$
-0.5	-0.000341	-34.18	37.14	1.0405
-1	-0.0022	-51.66		
-2	-0.00988	-88.78		
-3	-0.0178	-126.8		

(d) 9 w/cm^2

bias (volt)	I (mA)	$ln(\frac{-I}{1-e^{\left(\frac{-qV}{K_BT}\right)}})$	Slope (m)	$n = \frac{q}{slope.K_BT}$
-0.1	-0.0000019	-23.9	35.055	1.1
-0.6	-0.0000286	-40.491		
-1	-0.0000839	-54.394		
-1.4	-0.0001865	-69.59		

The figures below shows a plot of ln[-I/ (1 - exp(-qV/kT))] against reverse bias voltage for the fabricated devices, We can obtain the values of ideality factors n from the slopes (m) of linear portion of the graphs by substituting slopes values in eq.12

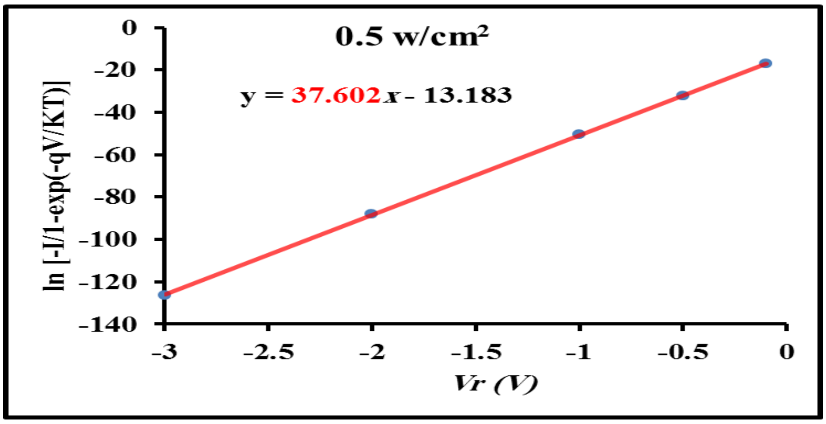

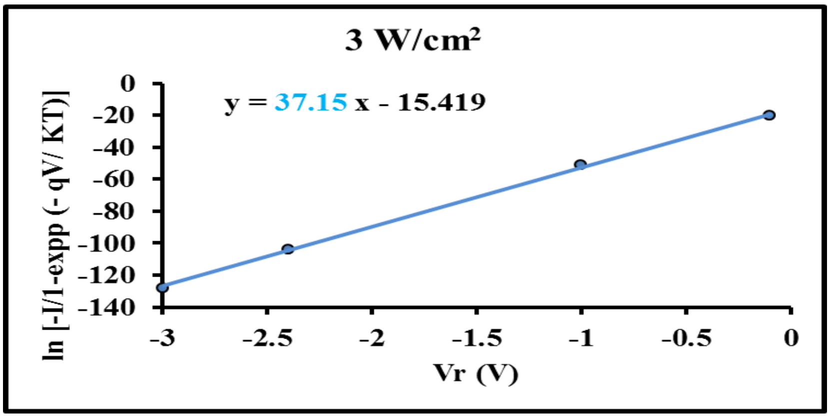

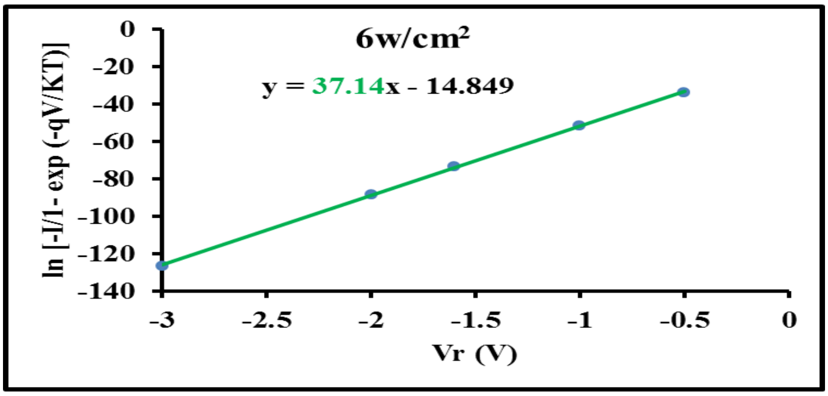

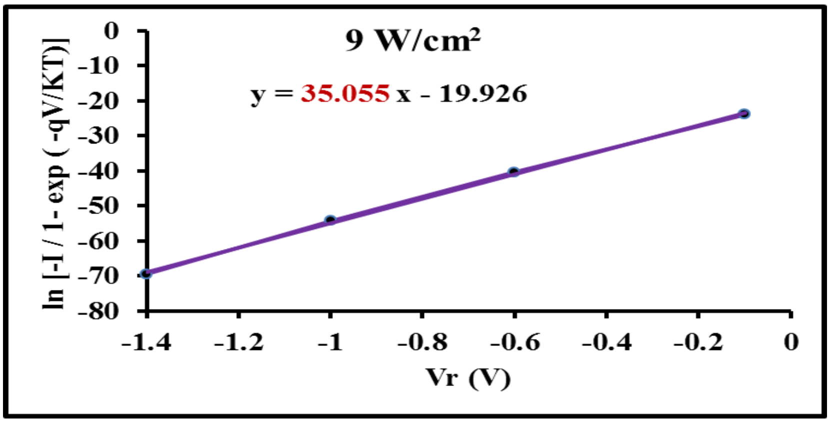

Figure (10): ln{-I/[1 exp (-qV /KB T)]} versus V plots for Al/pours –GaAs / n-GaAs/Al diodes , their porous layers were prepared using laser power densities of (a) 0.5 w/cm2 (b) 3 w/cm2 (c) 6 w/cm2 (d) 9 w/cm2, Schottky diodes from the reverse bias I–V data shown in Fig8.

4. Conclusion

In this paper , the effect of increasing laser power on the morphology of the porous layer in samples of (111) n-type GaAs was studied. The nanoparticles formed on the surfaces of the samples became smaller in size while the thickness of the porous layer increased with increasing laser power density , Porous GaAs/n–GaAs heterostructure with AL contact was investigated by means of the current–voltage characteristic in Al / Porous GaAs / n-GaAs/ Al structures which shows an improvement in the rectification property with increasing laser power densities during the preparation of the porous layer, This behavior is expected if we know that the photogenerated holes increased with increasing laser power density, which enhances the chemical dissolution process ,in other words, led to more difference in carriers density in the porous layer that were depleted due to caught by traps and a greater amount of carriers in the bulk layer. This difference in the density of carriers creates heterojunction, which is responsible for the rectification behavior.

REFERENCES

[1] Saxena D, Mokkapati S, Parkinson P, Jiang N, Gao Q, Tan H H, Jagadish (2013) Optically pumped room-temperature GaAs nanowire lasers. Nature Photonics 7: 963–968. DOI:10.1038/nphoton.2013.303

[2] V Kuzmin*, D Mokhov, T Berezovskaya, A Monastyrenko and A Bouravleuv (Electrochemical deposition of Ni on arrays of GaAs nanowires with n-type channels) V Kuzmin et al 2025 Nanotechnology 36 105601 Nanotechnology 36 (2025) 105601 (7pp).DOI 10.1088/1361-6528/ada2f2

[3] Xunjin Zhu,Electrical and Optoelectronic Properties Enhancement of n-ZnO/p-GaAs Heterojunction Solar Cells via an Optimized Design for Higher Efficiency Materials 2022, 15, 6268. doi.org/10.3390/ma15186268

[4] Ganjipour B, Wallentin J, Borgstrom MT, Samuelson L, Thelander C (Tunnel field-effect transistors based on InP-GaAs heterostructure nanowires). ACS Nano 6:3109–3113(2012) .DOI:10.1021/nn204838m

[5] Salehi, A. Nikfarjam, and D.J. Kalantari,(Pd/porous-GaAs Schottky contact for hydrogen sensing application), Sensors and Actuators B Chemical 113(1):419-427 (2006).DOI:10.1016/j.snb.2005.03.064

[6] G. Flamand and J. Poortmans,(Porous GaAs as a possible antireflective coating and optical diffusor for III–V solar cells) Phys. Stat. Sol. (a) 202, 1611-1615 (2005).doi.org/10.1002/pssa.200461199

[7] Martin PN, Aksamija Z, Pop E, Ravaioli U (Reduced thermal conductivity in nanoengineered rough Ge and GaAs nanowires). Nano Lett (2010) ,10:1120–1124 .doi.org/10.1021/nl902720v

[8] Dejarld MT, Shin JC, Chern W, Chanda D, Balasundaram K, Rogers JA, Li X (Formation of high aspect ratio GaAs nanostructures with metal assisted chemical etching). Nano Lett (2011), 11:49–54. DOI: 10.1021/nl202708d

[9] Nicholas Morgan, Vladimir G. Dubrovskii ,Ann-Kristin Stief,Didem Dede ,Marie Sanglé-Ferrière ,Alok Rudra ,Valerio Piazza andAnna Fontcuberta i Morral* (From Layer-by-Layer Growth to Nanoridge Formation: Selective Area Epitaxy of GaAs by MOVPE) Crystal Growth & Design 2023,Vol 23,Issue 7, 5083–5092. doi.org/10.1021/acs.cgd.3c00316

[10] Yana Suchikova,Sergii Kovachov, Zhakyp Karipbayev (Express Technology of Electrochemical Etching of Gallium Arsenide for the Formation of Massive Island Pores) 2023 IEEE 4th KhPI Week on Advanced Technology (KhPIWeek). DOI:10.1109/KhPIWeek61412.2023.10312896

[11] E.H. Sánchez-Martínez et al(Nonlocal Si δ-doping in horizontally-aligned GaAs nanowires) Surfaces and Interfaces 56 (2025) 105580. doi.org/10.1016/j.surfin.2024.105580

[12] Thomas B.O. Rockett et. al. (Growth of GaAsBi/GaAs multiple quantum wells with up to 120 periods) Journal of Crystal Growth Volume 589, 1 July 2022, 126679. doi.org/10.1016/j.jcrysgro.2022.126679

[13] Akio Higo, Takayuki Kiba, Junichi Takayama (Photoluminescence of In GaAs/GaAs Quantum Nanodisk in Pillar Fabricated by Biotemplate, Dry Etching and MOVPE Regrowth), ACS Appl. Electron. Mater. 2019, 1, 1945–19511947. DOI: 10.1021/acsaelm.9b00432

[14] L Cavigli 1, S Bietti, M Abbarchi, C Somaschini, A Vinattieri, M Gurioli, A Fedorov, G Isella, E Grilli, S Sanguinetti (Fast emission dynamics in droplet epitaxy GaAs ring-disk nanostructures integrated on Si) Journal of Physics: Condensed Matter. 2012 Vol 24(Issue10):104017. doi: 10.1088/0953-8984/24/10/104017.

[15] Sumit Sagar et. al.(High-efficiency GaAs solar cells with ordered nano-conical frustum arrays for enhanced light trapping and photovoltaic performance) Solar Energy ,Volume 288, (2025), 113299. doi.org/10.1016/j.solener.2025.113299

[16] Abdulmalik A. Madigawa ett, al, (Deterministic fabrication of GaAs-quantum-dot micropillar single-photon sources) (2025) ,physics. Optics.

[17] H. Villanti et al. (Self-assembled GaAs quantum dashes for direct alignment of liquid crystals on a III–V semiconductor surface) Applied Physics Express 18, 027001 (2025). DOI 10.35848/1882-0786/adb3eb

[18] A. Bakdid et.al. (Electronic and magnetic properties of quantum ring with two off-center donor atoms) Journal of Magnetism and Magnetic Materials,Volume 621, 2025, 172891. doi.org/10.1016/j.jmmm.2025.172891

[19] Suchikova et al (Formation of oxide crystallites on the porous GaAs surface by electrochemical deposition) Nanomaterials and Nanotechnology,(2022) Vol12 pp1–12 (30):184798042211273. DOI:10.1177/18479804221127307

[20] Xiaoying Huang et al.(Morphological engineering of aluminum droplet etched nanoholes for symmetric GaAs quantum dot epitaxy) 2020 Nanotechnology 31 495701. DOI 10.1088/1361-6528/abb1e9

[21] A. P. Oksanich, (Effect of Porous GaAs Layer Morphology on Pd/porous GaAs Schottky Contac) Journal of Nano- and Electronic Physics 2019, 11(5):05007. DOI:10.21272/jnep.11(5).05007

[22] Angélica Hernández et al (Optical properties of porous GaAs formed by low energy ion implantation), Vacuum Volume 171, 2020, 108976. doi.org/10.1016/j.vacuum.2019.108976

[23] H.S.Mavi,S.S.Islam,S.Rath,B.S.Chauhan,A.K.Shukla, (Laser-induced etching of Cr-O doped GaAs and wavelength dependent photoluminescence), Materials Chemistry and Physics Volume 86, Issues 2–3, 2004, Pages 414-419 doi.org/10.1016/j.matchemphys.2004.04.010

[24] B JOSHI (Wavelength dependent laser-induced etching of Cr–O doped GaAs: Morphology studies by SEM and AFM et al) Bull. Mater. Sci., Vol. 32, No. 1, 2009, pp. 31–35. © Indian Academy of Sciences. DOI:10.1007/s12034-009-0005-0

[25] H.S. Mavia*, A.K. Shuklaa, B.S. Chauhanb, S.S. Islamb (Surface morphology and formation of GaAs nanocrystals by laser-induced etching: SEM, PL and Raman studies) ,Materials Science and Engineering B107 (2004) 148-154. DOI:10.1016/j.mseb.2003.10.101

[26] H.S. Mavi a,*, S.S. Islam b, Rajesh Kumar a, A.K. Shukla (Spectroscopic investigation of porous GaAs prepared by laser-induced etching) Journal of Non-Crystalline Solids 352 (2006) 2236–2242. doi.org/10.1016/j.jnoncrysol.2006.02.046

[27] V. Svorcik, V. Rybka, V. Myslik,(Laser-stimulated etching of n-type semiconductors) Chem. Phys. Lett. Volume 144, Issues 5–6, Pages 548-551 (1988). doi.org/10.1016/0009-2614(88)87312-3

[28] V. Svorcik, V. Rybka, V. Myslik,(Photoetching of n-GaAs in Na+ and K+ salts) Chem. Phys. Lett. Volume 157, Issue 5, 1989, Pages 390-392. doi.org/10.1016/0009-2614(89)87268-9

[29] C. Veerender, M. Nagabhushanam, V. Haribabu(Dislocation-assisted complex scattering mobility of electrons in plastically deformed n-GaAs single crystals), Journal of Alloys and Compounds, Volume 204, Issues 1–2, February 1994, Pages 37-45. doi.org/10.1016/0925-8388(94)90069-8

[30] F.M. Ross, G. Oskam, P.C. Searson, J.M. Maculay, J.A. Liddle, (Crystallographic aspects of pore formation in gallium arsenide and silicon) Philosophical Magazine A 75(2) (1997) pp 525-539. DOI:10.1080/01418619708205156

[31] Emna Ben Amara,1 Amira Lebib,1 And Lotfi Beji (Structural and Electrical Investigation of Porous GaAs Layers on Different Crystallographically Oriented GaAs Substrates) Journal of Electronic Materials 49(9) (2020). doi.org/10.1007/s11664-020-08294-5

[32] H. Saghrouni a,⇑, A. Missaoui b, R. Hannachi a,b, L. Beji a,(Investigation of the optical and electrical properties of p-type porous GaAs structure) Superlattices and Microstructures 64 (2013) 507–517. doi.org/10.1016/j.spmi.2013.10.007

[33] H. Saghrouni a, R.Hannachi a, S.Jomni b, L.Beji a,n (Electrical investigation of the Au/n+–GaAs andAu/n-porous GaA sstructures) Phys. B 422, 64 (2013). DOI: 10.1016/j.physb.2013.04.038

[34] Amira Lebib,. Lotfi Beji, Nejeh Hamdaoui (Investigation of n-ZnO/p-porous GaAs/p-GaAs heterostructure for photodetection applications), Optical and Quantum Electronics 56(4) 2024. DOI:10.1007/s11082-023-06256-9